Broadband 90° hybrids based on Si_3N_4 multimode interference coupler

J. Mu,[1] K. Chen,[2] M. de Goede,[1] J. Yu,[2] M. Dijkstra,[1] S. He,[2,3] and S. M. García-Blanco[1]

[1] Optical Sciences Group, MESA+ Institute for Nanotechnology, University of Twente, P.O. Box 217, 7500 AE Enschede, The Netherlands, e-mail: j.mu@utwente.nl
[2] Centre for Optical and Electromagnetic Research, Zhejiang University, East Building No.5, Zijingang Campus, Hangzhou 310058, China
[3] Department of Electromagnetic Engineering, School of Electrical Engineering Royal Institute of Technology (KTH), S-100 44 Stockholm, Sweden

Optical 90° hybrids based on 2×4 multimode interference (MMI) coupler are designed and fabricated on a stripe Si_3N_4 layer. The hybrids show good performance on calculated parameters including excess loss, bandwidth and phase accuracy. The fabricated chips are characterized in a spectral window of 1520-1610 nm. The measured excess losses are below 1 dB while the common mode rejection ratios are within 10–20 dB. Lower than 10° phase error has been obtained over a bandwidth of 90 nm. The preliminary results show good agreement with the simulations.

Introduction

Stoichiometric silicon nitride (Si_3N_4), especially single-stripe layer, grown by low pressure chemical vapour deposition (LPCVD) has been reported to show tremendously low propagation loss (<0.1 dB/m at 1550 nm) and ultra-broad transparency window (from ~400 nm to 2350 nm) [1]. Recently, devices based on Si_3N_4 platform have been widely investigated such as telecommunications [2] and bio-sensing [3]. However, to our best knowledge, a 90° hybrid based on multimode interference [4] on Si_3N_4 has not been studied yet. The hybrids presented are mostly on silicon-on-insulator (SOI) platform for demodulating signals with quadrature phase shift keyed (QPSK) [5, 6], and also applied to current sensors [7]. Essentially, the relatively lower refractive index of Si_3N_4 (~2) brings lower mode phase errors and no shallowly etched waveguides are required [6]. In this paper, 90° Si_3N_4 hybrid is designed and preliminarily characterized. The measured losses and phase errors show good agreement with simulation, paving the way for further improvement and potential applications of the hybrid on Si_3N_4 platform.

Design and Simulation

Schematic of a 2 × 4 MMI hybrid are shown in Fig. 1. A single-stripe 200 nm thick Si_3N_4 layer grown by LPCVD is employed. The relevant substrate is 8 μm thick thermally oxidized SiO_2 and the cladding is ~6 μm thick plasma enhanced chemical vapor deposition (PECVD) SiO_2. The input and output ports are linearly tapered from 3 μm to 1.2 μm with a fixed length of 10 μm to ensure single-mode condition. They are further connected with adiabatic cosine S-bends to separate the input ports to match an input fiber array (i.e., 127 μm pitch), which is not shown here. At the wavelength of 1550 nm, the refractive indices of Si_3N_4 and

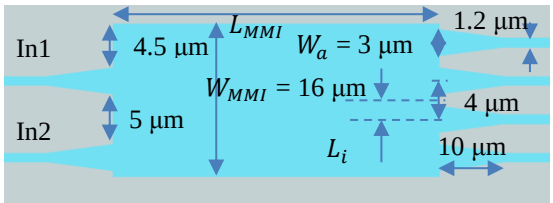

Fig. 1. Schematic of the 2×4 MMI hybrid. In1 and In2, and P1, P2, P3 and P4 denotes the input and output ports.

SiO_2 are 1.984 and 1.446 respectively. According to the self-imaging principle [4], the multiple confined modes in the multimode region of the MMI interfere together, providing a hybrid field at position L along the propagation direction. The field is expressed as

$$\psi(y,L)=\sum_{v=0}^{m-1}c_v\psi_v(y)\exp\left[i\frac{v(v+2)\pi}{3L_\pi}L\right] \quad (1)$$

where v is the mode order, m is the number of modes supported by the multimode region, c_v is the modal excitation coefficient, L is the propagation distance of the field inside the MMI section. The device is designed for transverse-electric (TE) applications. The width of MMI (W_{MMI}) is 16 μm which supports 10 TE modes with mode phase errors below 50°, which are a bit better than those with shallowly etched Si presented in [6] benefitting from the lower refractive index of Si_3N_4. The beat length (L_π) of MMI is calculated to be 368 μm.

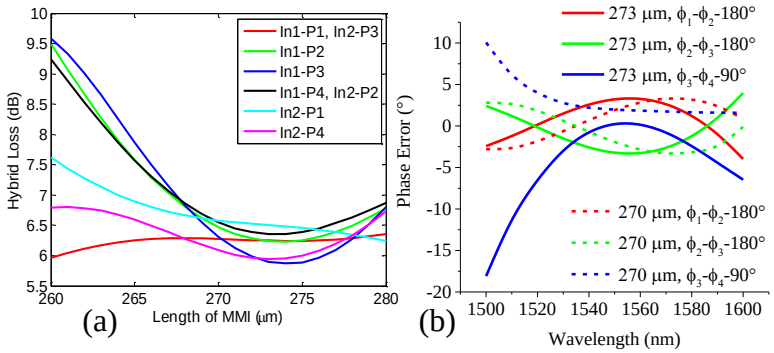

Fig. 2. α_h as a function of L_{MMI} for port (a) In1 and (b) In2. Phase errors between different output ports.

Fig. 2(a) show the hybrid loss (α_h) as a function of L_{MMI} with input port In1 and In2 respectively, which is calculated by propagating the eigen modes using equation (1) by a fast 2D mode solver (~second per calculation). The hybrid losses of the four output ports are lower than 7 dB, indicating less than 1 dB excess losses of the hybrid at L_{MMI} of 268–280 μm. Since most loss curves have a relatively low loss at L_{MMI} of ~273 μm. This length is smaller than the theoretical distance for 4-fold image patterning ($3L_\pi/4$) of 276 μm but it is regarded as an optimal value. The optimal parameters can be further determined by properly varying the port widths and locations as reported in the work of [8]. The lights from input port In1 and In2 are assumed to have the same amplitude and phase. Fig. 2(b) demonstrates phase errors between the output ports for the MMI including $\Delta\phi_1=\phi_1-\phi_4-180°$, $\Delta\phi_2=\phi_2-\phi_3-180°$ and $\Delta\phi_3=\phi_3-\phi_4-90°$, where ϕ_i (i = 1, 2, 3, 4) is a relative phase after removing changes of more than 2π extracted from the complex amplitude. The phase errors are all below 4° at L_{MMI} of 270 μm which is better than that at L_{MMI} of 273 μm. Therefore, devices with L_{MMI} of 270 μm are designed. Such 3D structure is further verified using 3D finite difference time domain (FDTD) at 1550 nm wavelength, and $\Delta\phi_1$, $\Delta\phi_2$ and $\Delta\phi_3$ are 1.85°, -1.80° and 3.0° respectively. Phase errors at other wavelengths of the spectrum range are found to be below 4° too.

Characterization Results

Chip characterization was carried out for the aforementioned 2 × 4 MMI hybrid integrated with an on-chip 1 × 2 MMI 3-dB splitter and 550 μm delay line in a spectrum range of 1520–1620 nm with a resolution of 0.1 nm. Fig. 3(a) and 5(b) show the spectrums as a function of wavelength with different scale. The total loss including 3-dB splitter and MMI hybrid, is interpreted by normalizing the peaks of the spectrum to the reference waveguide with highest transmission, as shown in Fig. 3(c). The standard deviation of the

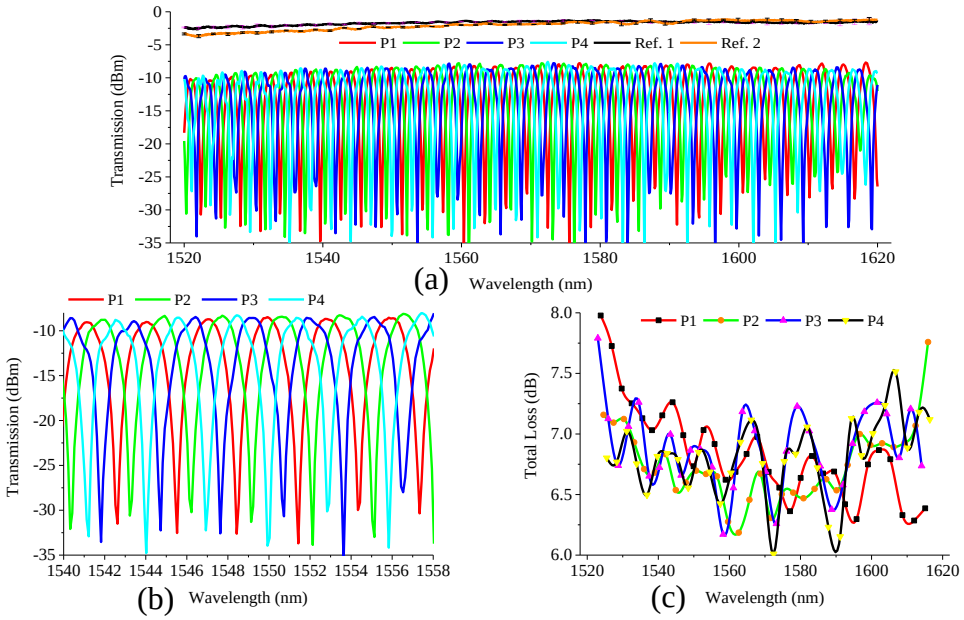

Fig. 3. (a) Transmission spectrum of the hybrid at L_{MMI} of 270 µm at wavelength range of 1520–1620 nm. (b) Zoom-in spectrum at 1540–1558 nm. (c) Normalized total loss of the device from measured peaks.

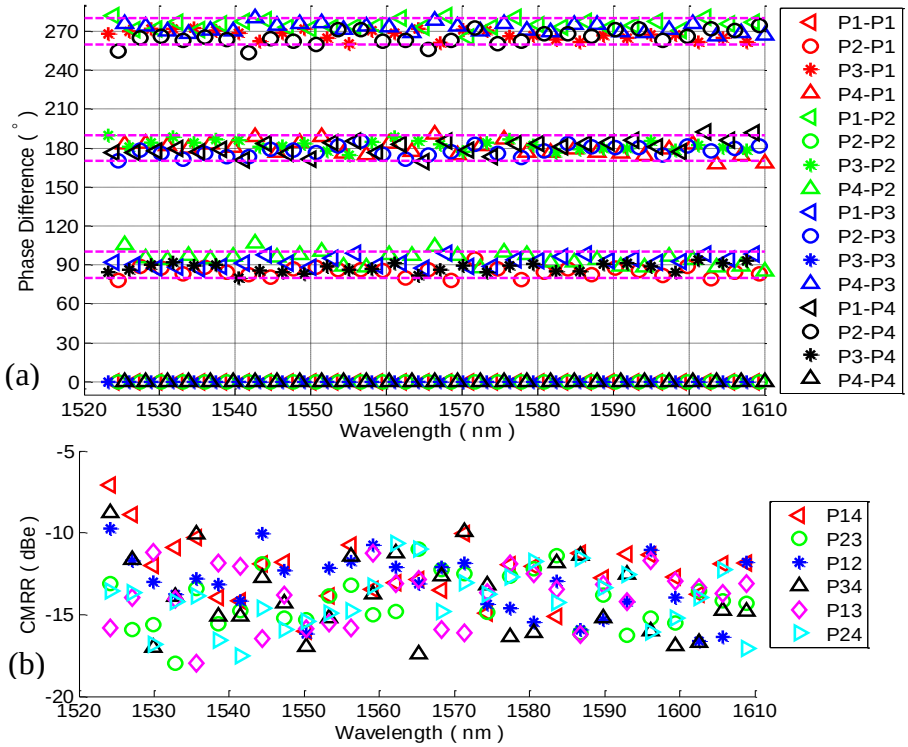

Fig. 4. (a) Phase difference extracted from measurements between the output ports by referring each output port. The dashed purple lines show 10° deviation to support the viewing. (b) The common mode rejection ratio (CMRR) between different output ports.

losses is below 0.4 dB which has already included the deviation of reference waveguide transmission after error propagation. It can be seen a large portion of the losses at different wavelength are between 6.5–7 dB, which agrees with the estimation above [Fig. 2(a)].

The relatively phase difference between the output ports ($\Delta\phi$) can be calculated from the related wavelength shift ($\Delta\lambda$) of the peaks, i.e. $\Delta\phi = 2\pi\Delta\lambda/\Delta\lambda_{FSR}$, where the peak distance ($\Delta\lambda_{FSR}$) is locally extracted. Fig. 4(a) shows the values of the phase difference related to different reference output port. For each reference output port, most phase difference stays within ±10° deviation corresponding to the target value (i.e. 90°, 180° and 270°) over the whole spectrum range. For example, for the reference output port P4, the measured phase error is below 6.5°, indicating good agreement with simulation. The variation mainly caused by fabrication uncertainties such as the width variation and roundness of the corners, which will be further explored in the future. In addition, the common mode rejection ratio (CMRR) is also investigated to evaluate how difference between output powers. It is calculated by $20\log_{10}[|P_i - P_j|/(P_i + P_j)]$ with a unit of dBe, where $P_{i,j}$ is the measured power of i- or j-th output port in Watt. The results illustrated in Fig. 4(b) as a function of the wavelength shows the CMRR mostly below -10 dB rather than below -20 dB as simulated. The reason is still under investigation.

Conclusion

In the work, an optical 90° MMI hybrid is presented. The device is simulated using both 2D mode solver and 3D FDTD. A preliminary characterization is carried out for the hybrid integrated with a 3-dB splitter at the MMI length of 270 μm in a spectrum range of 1520–1620 nm. The measured total losses at different output ports are mostly below 7 dB and located within 6.5–7 dB. Lower than 10° phase error is also achieved at different reference output ports over the whole spectrum range. Further optimizing of the design parameters is under investigating.

Acknowledgements

STW Perspectief program Memphis, under project number 13536.

References

[1] K. Wörhoff, R. G. Heideman, A. Leinse, and M. Hoekman, "TriPleX: a versatile dielectric photonic platform," *Advanced Optical Technologies*, vol. 4, pp. 189-207, Apr. 2015.

[2] L. Zhuang, M. Hoekman, C. Taddei, A. Leinse, R. G. Heideman, A. Hulzinga, et al., "On-chip microwave photonic beamformer circuits operating with phase modulation and direct detection," *Opt. Express*, vol. 22, pp. 17079-17091, 2014/07/14 2014.

[3] M. Boerkamp, T. van Leest, J. Heldens, A. Leinse, M. Hoekman, R. Heideman, et al., "On-chip optical trapping and Raman spectroscopy using a TripleX dual-waveguide trap," *Opt. Express*, vol. 22, pp. 30528-30537, 2014/12/15 2014.

[4] L. B. Soldano and E. C. M. Pennings, "Optical multi-mode interference devices based on self-imaging: principles and applications," *J. Lightwave Technol.*, vol. 13, pp. 615-627, Apr. 1995.

[5] S. H. Jeong and K. Morito, "Novel Optical 90° Hybrid Consisting of a Paired Interference Based 2×4 MMI Coupler, a Phase Shifter and a 2×2 MMI Coupler," *J. Lightwave Technol.*, vol. 28, pp. 1323-1331, 2010.

[6] R. Halir, G. Roelkens, A. Ortega-Moñux, and J. G. Wangüemert-Pérez, "High-performance 90° hybrid based on a silicon-on-insulator multimode interference coupler," *Opt. Lett.*, vol. 36, pp. 178-180, 2011/01/15 2011.

[7] S.-M. Kim, W.-S. Chu, S.-G. Kim, and M.-C. Oh, "Integrated-optic current sensors with a multimode interference waveguide device," *Opt. Express*, vol. 24, pp. 7426-7435, 2016/04/04 2016.

[8] J. Mu, S. A. Vázquez-Córdova, M. A. Sefunc, Y. S. Yong, and S. M. G. Blanco, "A Low-Loss and Broadband MMI-Based Multi/Demultiplexer in Si_3N_4/SiO_2 Technology," J. Lightwave Technol., vol. 34, pp. 3603-3609, 2016.